ATMOSPHERIC SCIENCE LETTERS
Atmos. Sci. Let. **17**: 548–555 (2016)
Published online 31 August 2016 in Wiley Online Library
(wileyonlinelibrary.com) **DOI:** 10.1002/asl.691

RMetS
Royal Meteorological Society

Changes in marine fog in a warmer climate

Hideaki Kawai,[1]* Tsuyoshi Koshiro,[1] Hirokazu Endo,[1] Osamu Arakawa[2] and Yuichiro Hagihara[3]

[1]*Meteorological Research Institute, Japan Meteorological Agency, Tsukuba, Japan*
[2]*Faculty of Life and Environmental Sciences, Universitiy of Tsukuba, Tsukuba, Japan*
[3]*Earth Observation Research Center, Japan Aerospace Exploration Agency, Tsukuba, Japan*

**Correspondence to:*
H. Kawai, Meteorological Research Institute, Japan Meteorological Agency, 1-1 Nagamine, Tsukuba, Ibaraki 305-0052, Japan.
E-mail: h-kawai@mri-jma.go.jp

Received: 15 April 2016
Revised: 30 June 2016
Accepted: 1 August 2016

Abstract

Changes in marine fog in a warmer climate are investigated through simulations using the atmospheric component of a global climate model, with both observed and perturbed sea surface temperature forcing. Global changes in marine fog occurrence in different seasons are compared. We show that the changes in marine fog occurrence correspond well to changes in horizontal temperature advection near the surface in a warmer climate. Therefore, the changes in marine fog can be well explained by large-scale circulation changes. Regarding changes in the characteristics of marine fog, we show that the in-cloud liquid water content of marine fog is consistently increased in a warmer climate, for a given horizontal surface temperature advection. It is also confirmed that the contribution of changes in marine fog to cloud feedback is not negligible, but is small.

Keywords: **marine fog; climate change; large-scale circulation; low cloud feedback**

1. Introduction

Marine fog (Koračin *et al.*, 2014), especially over the mid-latitude ocean, is an important target in climate simulation because it affects maritime traffic and because sky-obscuring marine fog is an important contributor to the Earth's radiation budget due to its widespread coverage. The purpose of this study is to reveal global-scale changes in marine fog in a warmer climate.

Many studies have investigated the global distribution of marine fog and the basic meteorological factors that primarily determine its distribution. Klein and Hartmann (1993) reported a global distribution of sky-obscuring marine fog obtained by shipboard observations (Warren *et al.*, 1988), and noted the importance of surface warm air advection in determining the distribution. Several studies followed, including Norris (1998a, 1998b) and Norris and Klein (2000), who compared and analyzed the meteorological fields related to fog and other cloud regimes, and Koshiro and Shiotani (2014) proposed a stability index related to fog distribution. In addition, Kawai *et al.* (2015) showed that the occurrence of clouds below 240 m globally, estimated from satellite lidar, has a high correlation with the temperature difference between a height of 2 m and the sea surface, which is controlled primarily by warm air advection.

Recently, changes in low cloud in a warmer climate and low cloud feedback have been studied extensively, especially with respect to tropical and subtropical low cloud (e.g., Kawai, 2012; Blossey *et al.*, 2013; Brient and Bony, 2013; Webb and Lock, 2013; Zhang *et al.*, 2013; Bretherton and Blossey, 2014). However, there have been few studies related to changes and cloud feedback in mid-latitude low cloud, and even fewer such studies of mid-latitude marine fog.

The objective of our study is to discuss the change in marine fog in a warmer climate. In order to simplify the discussion of the mechanism and isolate the cloud feedback of marine fog, we use simulation data from AMIP [atmospheric models, forced by observed sea surface temperature (SST)] and AMIP with increased SST experiments. We comprehensively discuss changes in marine fog in a warmer climate, changes in meteorological fields that cause the marine fog changes, changes in the characteristics of marine fog, and the impact of changes in marine fog on cloud feedback.

2. Data

2.1. Model data

Under the fifth phase of the Climate Model Intercomparison Project (CMIP5) (Taylor *et al.*, 2012) and the Cloud Feedback Model Intercomparison Project Phase-2 (CFMIP2) (Bony *et al.*, 2011), we performed simulations of type AMIP (labeled as amip), and AMIP with SST increased by 4 K with uniform perturbations (amip4K) and with a composite pattern obtained from CMIP3 models (amipFuture). The model runs are 31 years in length (1979–2009). These AMIP series simulations are often used for studies related to cloud feedback; e.g., Webb and Lock (2013) and Webb *et al.* (2014).

We ran these simulations using MRI-CGCM3 (Yukimoto *et al.*, 2011, 2012), which has 48 vertical levels in total, and 5 levels below 910 hPa with a lowest layer of thickness 10 hPa. The model level data are used, and

both monthly and daily average data are used in the analysis. In addition, CMIP5 multi-model data for sea level pressure (SLP) are used (the models used are listed in Table S1, Supporting information) to examine the robustness of circulation changes in MRI-CGCM3.

2.2. Observation data

Shipboard observation data for 1954–2008 from the Extended Edited Cloud Report Archive (EECRA) (Hahn and Warren, 2009) are used to examine the representation of marine fog in the model simulation. In addition, we used fog or near-surface cloud frequency data, obtained from C2 data of the Kyushu University (KU) cloud mask product (Hagihara *et al.*, 2010), retrieved from Cloud–Aerosol Lidar and Infrared Pathfinder Satellite Observation (CALIPSO) (Winker *et al.*, 2009) data for 2007–2009.

3. Basic features of model marine fog

3.1. Marine fog in the model and observations

First, to examine the representation of marine fog in the model, the simulation data are compared with the shipboard and satellite observations (see Kawai *et al.* (2015) for details). Regarding the satellite cloud mask data, fog is defined as cloud at heights lower than 240 m, and the fog-occurrence frequency derived from the cloud mask data is a lower limit of the estimate, because CALIPSO cannot observe clouds that occur below thick cloud (Kawai *et al.*, 2015). Teixeira (1999) calculated fog occurrence in a model as the occurrence of cloud water content greater than $0.016\,\mathrm{g\,kg^{-1}}$ at the lowest model level. However, in this study we simply define fog frequency as the cloud fraction at the lowest model level because in-cloud liquid water content (LWC) typically exceeds $0.1\,\mathrm{g\,kg^{-1}}$ (shown later in Figure 5), which is much larger than the threshold of $0.016\,\mathrm{g\,kg^{-1}}$, and it is confirmed in a preliminary comparison that fog frequency calculated from cloud fraction and the method using a cloud water content threshold gives similar results. In addition, the cloud fraction output calculated in the model is temporally averaged for each model timestep. Therefore, the data provide an appropriate climatology of fog occurrence even if the diurnal variation is large.

Figure 1 shows that these three climatologies of fog-occurrence frequency (MRI-CGCM3 simulation, shipboard and satellite observations), which are totally independent, are consistent. In July, marine fog is frequent around Kamchatka Peninsula, near Newfoundland, north of Iceland, and in the Arctic Ocean north of Eurasia, in all three climatologies. Although the numbers of shipboard observations are insufficient over the Southern Ocean, fog frequencies in model data and satellite observations are similar in this region. In January, the common fog areas are the Northeastern Pacific and the Southern Ocean in all three climatologies, and both the model simulation and the satellite data show fog occurrence over the Arctic Ocean. Spatial anomaly correlation and root mean square error against shipboard climatology were calculated monthly for 10 CMIP5 multi-model data. It turned out that MRI-CGCM3 has the highest annual mean score of spatial anomaly correlation (0.70) and the third least root mean square error. In addition, about half of models failed to capture the observed fog distribution except for boreal summer. Based on the comparison and the scores, we conclude that MRI-CGCM3 represents fog relatively well and that the model data are suitable for use in studies of the future changes, at least in a qualitative sense.

3.2. Vertical cloud structures in the model

Figure 2 shows composites of the vertical structures of clouds and relative humidity in the model over the North Pacific in July based on daily data for southerly ($V > 2\,\mathrm{m\,s^{-1}}$) and northerly ($V < -2\,\mathrm{m\,s^{-1}}$) surface wind. When the surface wind is southerly (Figure 2(a) and (c)), the contours of potential temperature are tilted near the surface, which denotes a stable boundary layer, relative humidity is high, and the clouds touch the sea surface around 40°–50°N. This clearly shows that the model represents warm air advection fog, where warm surface air is cooled by cold SST and the water vapor is condensed, as the mechanism is discussed by many studies (e.g., Klein and Hartmann, 1993). On the other hand, when the surface wind is northerly (Figure 2(b) and (d)), the contours of potential temperature are upright near the surface, which denotes a well-mixed boundary layer, relative humidity is lower, and the clouds do not touch the sea surface around 40°–50°N. This means that fog rarely appears when the wind is northerly in the model and floating low clouds instead tend to appear. These features are consistent with shipboard cross-section observations in the North Pacific, including those reported by Tanimoto *et al.* (2009).

4. Results

4.1. Changes in marine fog

In July, the occurrence of marine fog (cloud fraction at the lowest model level) is reduced in the amip4K simulation in the central North Pacific and the western North Atlantic near Newfoundland (Figure 3(c)). The maximum reduction reaches 6%. On the other hand, the occurrence of marine fog is increased by up to 3% in the eastern North Pacific (south of Alaska). In January, a dipole feature is found in the eastern North Pacific, which corresponds to an area of frequent fog occurrence: fog decreases in the western part by up to 6% and increases in the eastern part of this area by up to 3% (Figure 3(d)). Similar results are seen in the difference between amipFuture and amip (Figure 3(e,f)). Thus, these changes are robust for a warmer climate regardless of the pattern of SST increase.

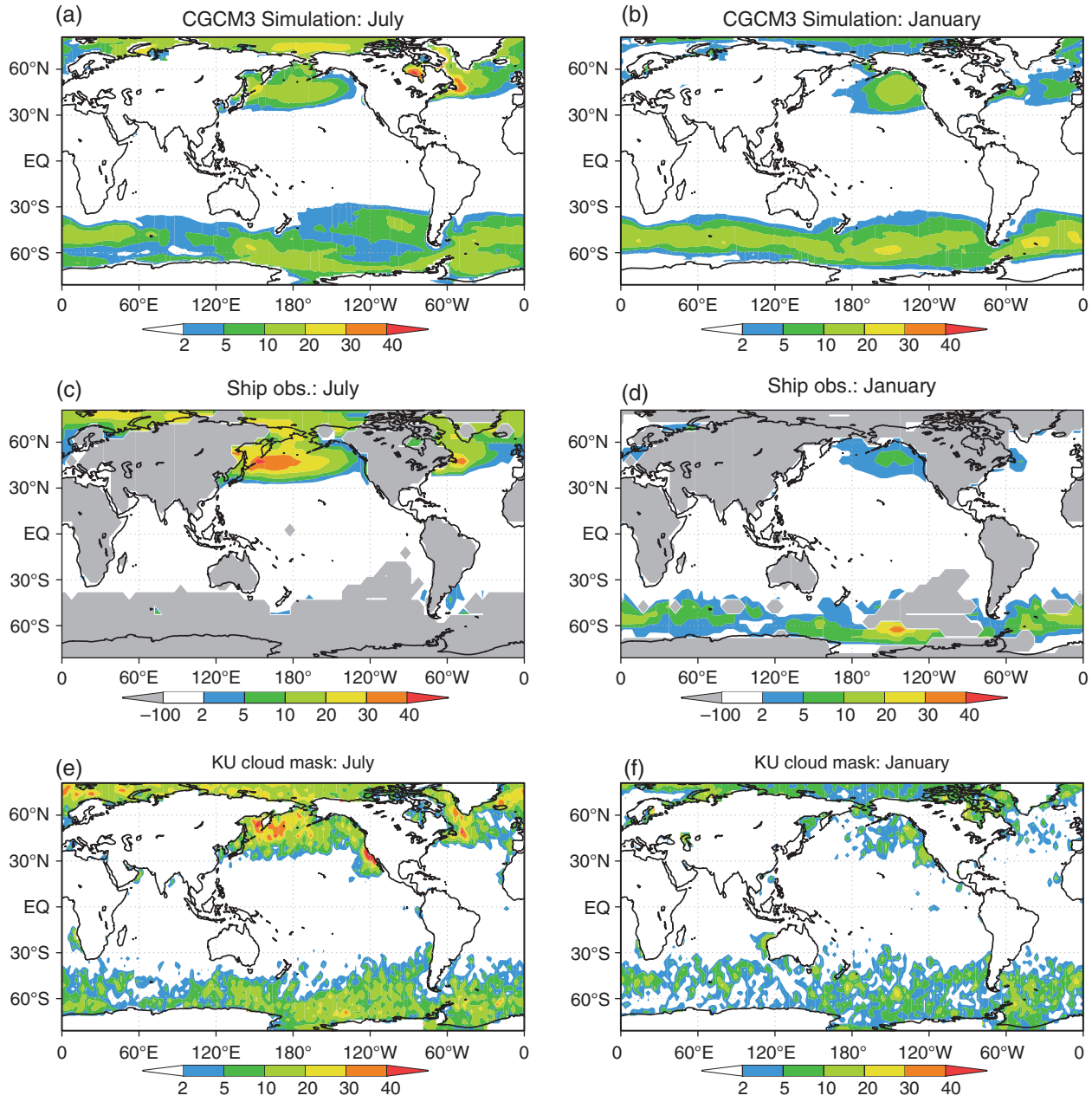

Figure 1. (a,b) Cloud fraction at the lowest model level in the MRI-CGCM3 simulation (1979–2009). (c,d) Shipboard fog observational climatology (1954–2008) on a 5° × 5° grid, where grid points are shaded gray if the sample number is <100. (e,f) Occurrence frequency of fog (2007–2009) derived using the KU cloud mask (0–240 m bin). Units are %; data are shown for July (left panels) and January (right panels).

4.2. Changes in meteorological fields

To understand changes in marine fog occurrence, changes in meteorological fields are examined. Changes in SLP are shown in Figure 4(c) and (d). In July, subtropical high-pressure systems occur in the North Pacific and the North Atlantic (Figure 4(a)), and western parts of these high-pressure systems correspond to areas of frequent fog occurrence, where southerly winds are dominant. In a warmer climate, the high-pressure system in the North Pacific is weakened between 180° and 150°W, which corresponds to weakened southerly winds in the central North Pacific and strengthened southerlies in the eastern North Pacific. Therefore, surface temperature advection, which is calculated from 10 m wind and SST (Klein *et al.*, 1995), is decreased in the central North Pacific and increased in the eastern North Pacific (Figure 4(e)). This pattern is consistent with the reduction in marine fog in the central North Pacific and the increase in the eastern North Pacific. Note that locations with maximum changes in fog occurrence correspond to the poleward side of locations with large changes in surface temperature advection because climatological relative humidity near surface is larger (closer to saturation) at higher latitude (see Figure 2(c,d)) and fog occurrence is more sensitive to warm air advection there. The low-pressure area over the North American continent is weakened

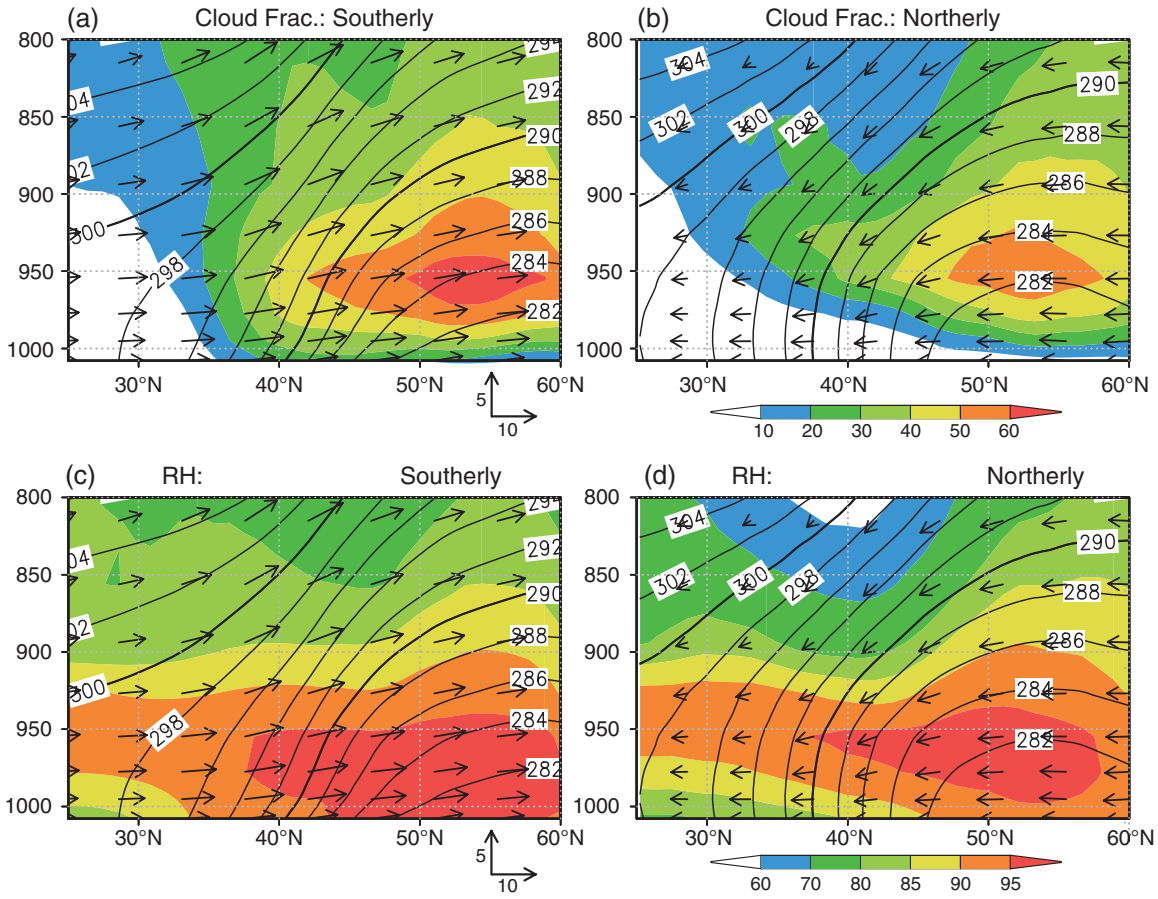

Figure 2. Vertical structure of clouds (a,b) and relative humidity (c,d) in MRI-CGCM3. Composites of daily data where the surface wind is (a,c) southerly ($V > 2\,m\,s^{-1}$) and (b,d) northerly ($V < -2\,m\,s^{-1}$) are shown. The data are averaged between 170°E and 170°W for July (1979–2009). Shading shows cloud fraction (%), contours show potential temperature (K), horizontal arrows show meridional wind ($m\,s^{-1}$), and vertical arrows show vertical wind ($-hPa\,h^{-1}$). Vertical axis is pressure (hPa).

in a warmer climate, which corresponds to reductions in southerly wind strength and temperature advection near Newfoundland. This is also consistent with a local reduction in marine fog. In January, the area of frequent fog occurrence corresponds to the eastern part of the Aleutian low-pressure system (Figure 4(b)). In a warmer climate, a negative SLP anomaly occurs off the west coast of the United States, which corresponds to a decrease (increase) in southerly wind on the western (eastern) side of the anomaly. This pattern explains the dipole pattern in marine fog changes in the eastern North Pacific in January. In the Southern Ocean, marine fog occurrence is reduced along 40°S and increased along 60°S, and this can be attributed to decreases and increases in temperature advection along 40° and 60°S, respectively (Figure S1). In January, the changes in marine fog occurrence over the Southern Ocean have a more zonally uniform structure than in July, and this is consistent with more zonally uniform changes in the SLP pattern during this month.

To confirm the robustness of the changes in SLP, CMIP5 multi-model data are compared (Figure S2). The analysis confirms all the characteristics of changes in SLP mentioned above, including a weakened high-pressure system in the central North Pacific and a weakened low-pressure area over the North American continent in July, a negative anomaly off the west coast of the United States in January, and more zonally uniform changes in SLP over the Southern Ocean in January than in July. In addition, these changes are quite similar in the amip4K and amipFuture simulations. Therefore, we can conclude that these changes are robust and deserving of analysis and discussion. The weakening of the high-pressure system in the central North Pacific and weakening of the low-pressure area over the North American continent in July could be explained by weakened monsoon circulations in a warmer climate (e.g., Tanaka *et al.*, 2005; Kitoh *et al.*, 2013), which would weaken SLP contrasts between land and ocean. The increase in SLP around 45°S can be attributed to a poleward shift of the jet in a warmer climate (e.g., Medeiros *et al.*, 2015). The similarity of the patterns of SLP changes in the amip4K and amipFuture simulations suggests that the main factor for the SLP changes is stabilization of troposphere because of SST increase and consequent weakening of major overturning circulations, including Hadley, Walker and monsoon circulations.

Sugimoto *et al.* (2013) discussed trends in fog frequency in recent decades observed in coastal land areas adjacent to the North Pacific, into which advection fog frequently flows. They found that decreases in fog in

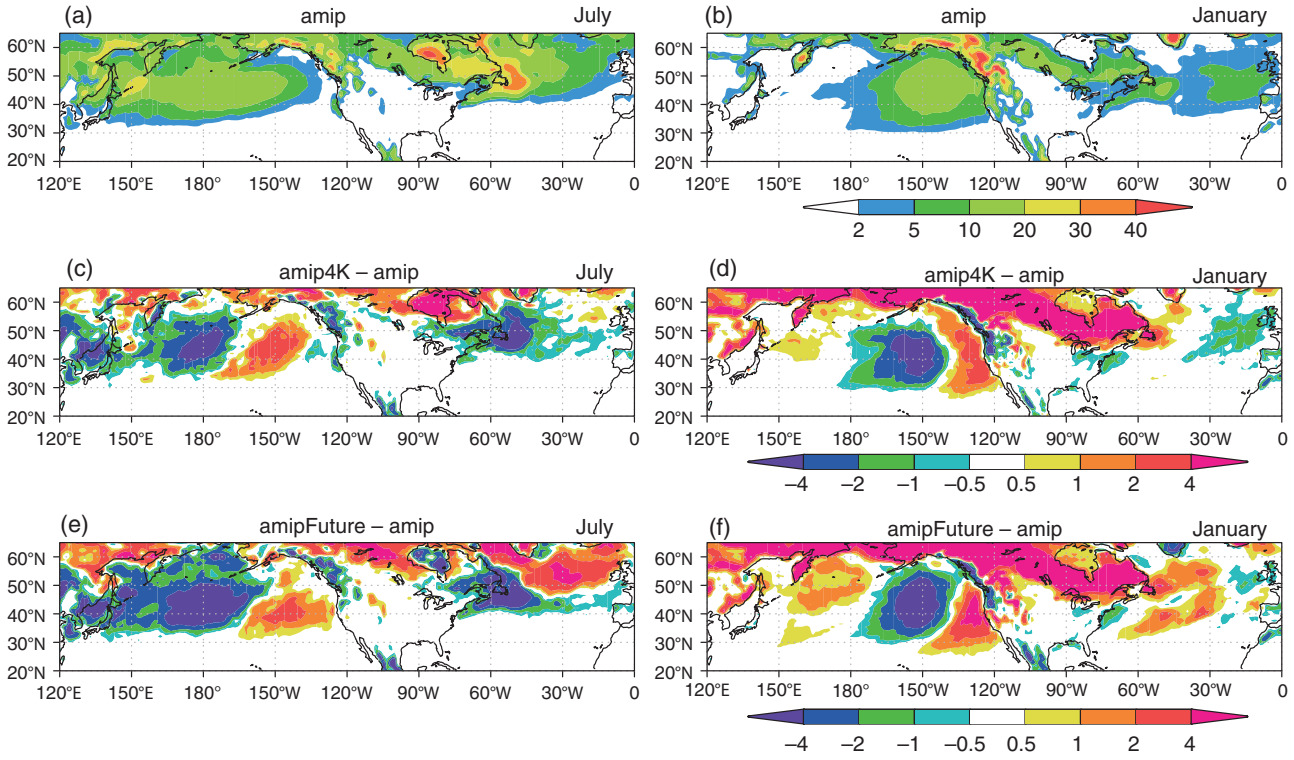

Figure 3. (a,b) Climatology of marine fog (cloud fraction at the lowest model level) in MRI-CGCM3, and the change from (c,d) amip to amip4K, and (e,f) amip to amipFuture. Units are %; data are shown for July (left panels) and January (right panels).

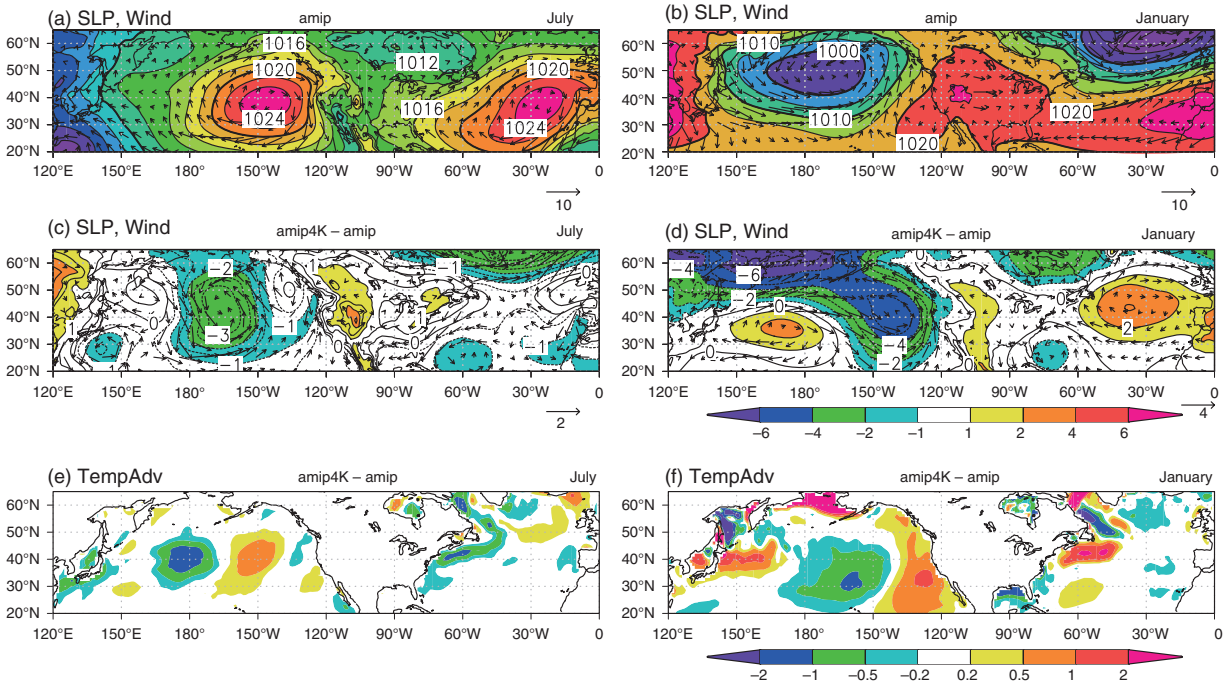

Figure 4. (a,b) Climatology of sea level pressure (hPa) and 10 m wind ($m\,s^{-1}$) in MRI-CGCM3, and (c,d) the change from amip to amip4K. (e,f) Change in surface temperature advection ($K\,day^{-1}$) from amip to amip4K. Data are shown for July (left panels) and January (right panels).

recent decades correspond to reductions in warm air advection. It is shown in this study that changes in marine fog correspond well to changes in horizontal temperature advection near the surface in a warmer climate. This suggests that the changes in marine fog can be well explained by large-scale circulation changes. There are numerous studies related to Californian coastal fog in summer, and for instance, Johnstone and Dawson (2010) showed relationships among the fog frequency, SLP, meridional wind, and SST, on both interannual and interdecadal timescales. However, note that there is a difference in the mechanisms of fog

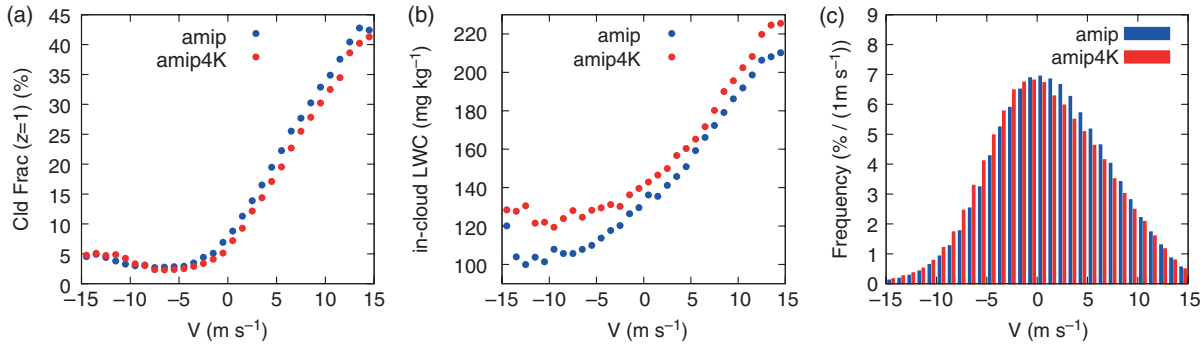

Figure 5. Relationships between meridional surface wind and (a) cloud fraction and (b) in-cloud liquid water content, at the lowest model level. (c) Meridional surface wind frequency histogram. Daily data of every single grid is binned into meridional surface wind bins of 1 m s^{-1} interval, and averaged over the North Pacific (160°E – 160°W, 40 – 50°N), for July (1979–2009). Blue and red dots/bars show amip and amip4K data, respectively.

occurrence between Californian coastal fog, which is significantly affected by the coastal topography including ocean upwelling and offshore air flow, and advection marine fog, which occurs over broad areas in mid-latitude global oceans.

4.3. Relationship between surface wind and fog

Figure 5(a) shows the relationship between meridional surface wind and cloud fraction at the lowest model level (i.e., fog frequency) over the North Pacific (160°E – 160°W, 40 – 50°N), using daily data for July (1979–2009). It is clear that cloud fraction increases as the southerly wind increases, and the slope of the relationship is 2.7%/(m s^{-1}) for the wind speed 0–10 m s^{-1}. This slope can quantitatively explain that the peak values of positive and negative changes in fog frequency in the North Pacific are +3 and −6% (Figure 3(c)) and the corresponding changes in meridional wind are +1 and −2 m s^{-1}, respectively (Figure 4(c)). Figure 5(b) shows a similar relationship between meridional wind and in-cloud LWC, which is LWC in a grid divided by the cloud fraction, at the lowest model level. It is also clear that in-cloud LWC increases as the southerly wind increases. In a warmer climate, in-cloud LWC is increased for a given meridional wind. This means that the optical thickness of fog could increase for a given meridional wind in a warmer climate, unless the cloud droplet number concentration decreases substantially. The increase in in-cloud LWC can be explained by air masses that have larger specific humidity in a warmer climate, and can therefore condense out more water vapor for a given rate of temperature advection, as approximately corresponds to a given meridional wind. Similar characteristics are found over the Southern Ocean (0° – 360°E, 45° – 60°S), although the wind is in the opposite direction (Figure S3).

4.4. Impact of changes in marine fog on cloud feedback

The contribution of changes in marine fog to cloud feedback in the model is now briefly examined. The approximate cloud radiative effect (W m^{-2}) of clouds between the surface z_0 and height z for upward shortwave radiation, CRE_SW↑$(z-z_0)$, is estimated as follows:

$$\begin{aligned}&\mathrm{CRE\_SW}\uparrow(z-z_0)\\&\quad\approx(\mathrm{SW}\uparrow(\text{all sky},z)-\mathrm{SW}\uparrow(\text{clear sky},z))\\&\quad-\left(\mathrm{SW}\uparrow(\text{all sky},z_0)-\mathrm{SW}\uparrow(\text{clear sky},z_0)\right),\end{aligned}$$

where SW↑ denotes the upward shortwave radiative flux (the sign is positive for downward). The contribution of clouds between z_0 and z to shortwave cloud feedback can be roughly estimated from the difference in CRE_SW↑$(z-z_0)$ between the amip4K and amip simulations. Changes in CRE_SW↑$(z-z_0)$ due to clouds between the surface and 960, 900 and 700 hPa are examined. For example, it is clear from Figure S4 that the geographical pattern of change in CRE_SW↑$(z-z_0)$ between the surface and 960 hPa essentially corresponds to the change in marine fog occurrence shown in Figure 3 for July. Changes in CRE_SW↑$(z-z_0)$ are positive in areas with reduced fog, such as the central North Pacific and the western North Atlantic, and changes are negative in areas with increased fog, such as the eastern North Pacific. However, these geographical patterns become less clear for changes in CRE_SW↑$(z-z_0)$ between the surface and 900 hPa, and changes between the surface and 700 hPa show quite different geographical patterns and much larger amplitudes compared with the case between the surface and 960 hPa. This means that the impact of changes in marine fog on cloud feedback is not negligible, but is small, and that the contribution of low clouds, in an atmospheric layer higher than fog, dominates for low-cloud feedback.

5. Summary

Changes in marine fog over the global mid-latitude ocean in a warmer climate, which have received relatively little attention to date, were investigated in this study, using AMIP and AMIP with increased SST experiments. It was confirmed that simulated global

marine fog occurrence is represented relatively well in MRI-CGCM3, by comparison with two independent global observation datasets. The vertical structures of marine fog represented in the model were briefly discussed by showing composite cases corresponding to southerly and northerly winds.

Simulated global changes in marine fog occurrence in different seasons were compared, and changes in SLP were also examined. An important conclusion of this study is that the changes in marine fog correspond well to changes in horizontal temperature advection near the surface in a warmer climate in the simulations. The results suggest that large-scale changes in marine fog can be well explained by large-scale circulation changes.

Regarding changes in characteristics of marine fog, it was shown that in-cloud LWC of marine fog is consistently increased in a warmer climate for a given meridional wind; i.e., for a given horizontal surface temperature advection. In addition, it was confirmed that the contribution of the changes in marine fog to cloud feedbacks is not negligible, but is small.

Robust, general characteristics of the changes in marine fog are discussed in this study. However, it is possible that the vertical resolution of climate models is not high enough to capture more detailed characteristics of changes in marine fog in a warmer climate (the lowest model layer is about 85 m in MRI-CGCM3). Therefore, simulations using models with higher vertical resolution would be desirable to reveal more detailed changes in marine fog, in a future study. In addition, representations of fog distribution of CMIP5 multi-model data will be examined and the changes in a warmer climate will be studied in detail in future research.

Acknowledgements

The EECRA data were obtained from the Carbon Dioxide Information Analysis Center, Oak Ridge National Laboratory, U.S. Department of Energy. The contact person for requesting the KU cloud mask data used in this study is Hajime Okamoto (okamoto@riam.kyushu-u.ac.jp). This research was supported in part by 'the Program for Risk Information on Climate Change' and 'the Social Implementation Program on Climate Change Adaptation Technology', both of the Ministry of Education, Culture, Sports, Science and Technology (MEXT), Japan, and by the Environment Research and Technology Development Fund (2-1503) of the Ministry of the Environment. We acknowledge the two anonymous reviewers for their constructive and insightful comments. We thank Shuhei Maeda for valuable discussions. Figures were edited by Rikako Matsumoto.

Supporting information

The following supporting information is available:

Appendix S1. Abbreviations, experiment names, and terminologies.

Figure S1. Changes in marine fog occurrence and sea level pressure in the southern hemisphere.

Figure S2. Changes in sea level pressure simulated by the CMIP5 multi-model ensemble.

Figure S3. Relationships between meridional wind and cloud fraction, and in-cloud liquid water content over the Southern Ocean.

Figure S4. Changes in the approximate cloud radiative effect.

Table S1. List of CMIP5 models used for Figure S2.

References

Blossey PN, Bretherton CS, Zhang M, Cheng A, Endo S, Heus T, Liu Y, Lock AP, De Roode SR, Xu KM. 2013. Marine low cloud sensitivity to an idealized climate change: the CGILS les intercomparison. *Journal of Advances in Modeling Earth Systems* **5**(2): 234–258, doi: 10.1002/jame.20025.

Bony S, Webb M, Bretherton CS, Klein SA, Siebesma P, Tselioudis G, Zhang M. 2011. CFMIP: towards a better evaluation and understanding of clouds and cloud feedbacks in CMIP5 models. *Clivar Exchanges* **56**: 20–22.

Bretherton CS, Blossey PN. 2014. Low cloud reduction in a greenhouse-warmed climate: results from Lagrangian LES of a subtropical marine cloudiness transition. *Journal of Advances in Modeling Earth Systems* **6**(1): 91–114, doi: 10.1002/2013MS000250.

Brient F, Bony S. 2013. Interpretation of the positive low-cloud feedback predicted by a climate model under global warming. *Climate Dynamics* **40**(9–10): 2415–2431, doi: 10.1007/s00382-011-1279-7.

Hagihara Y, Okamoto H, Yoshida R. 2010. Development of a combined CloudSat-CALIPSO cloud mask to show global cloud distribution. *Journal of Geophysical Research* **115**: D00H33, doi: 10.1029/2009JD012344.

Hahn CJ, Warren SG. 2009. *Extended Edited Synoptic Cloud Reports From Ships and Land Stations Over the Globe, 1952–1996 (2009 Update). NDP-026C*. Carbon Dioxide Information Analysis Center, Oak Ridge National Laboratory: Oak Ridge, TN.

Johnstone JA, Dawson TE. 2010. Climatic context and ecological implications of summer fog decline in the coast redwood region. *Proceedings of the National Academy of Sciences of the United States of America* **107**(10): 4533–4538, doi: 10.1073/pnas.0915062107.

Kawai H. 2012. Examples of mechanisms for negative cloud feedback of stratocumulus and stratus in cloud parameterizations. *SOLA* **8**: 150–154, doi: 10.2151/sola.2012-037.

Kawai H, Yabu S, Hagihara Y, Koshiro T, Okamoto H. 2015. Characteristics of the cloud top heights of marine boundary layer clouds and the frequency of marine fog over mid-latitudes. *Journal of the Meteorological Society of Japan* **93**: 613–628, doi: 10.2151/jmsj.2015-045.

Kitoh A, Endo H, Krishna Kumar K, Cavalcanti IFA, Goswami P, Zhou T. 2013. Monsoons in a changing world: a regional perspective in a global context. *Journal of Geophysical Research [Atmospheres]* **118**(8): 3053–3065, doi: 10.1002/jgrd.50258.

Klein SA, Hartmann DL. 1993. The seasonal cycle of low stratiform clouds. *Journal of Climate* **6**: 1587–1606, doi: 10.1175/1520-0442(1993)006<1587:TSCOLS>2.0.CO;2.

Klein SA, Hartmann DL, Norris JR. 1995. On the relationships among low-cloud structure, sea surface temperature, and atmospheric circulation in the summertime Northeast Pacific. *Journal of Climate* **8**: 1140–1155.

Koračin D, Dorman CE, Lewis JM, Hudson JG, Wilcox EM, Torregrosa A. 2014. Marine fog: a review. *Atmospheric Research* **143**: 142–175, doi: 10.1016/j.atmosres.2013.12.012.

Koshiro T, Shiotani M. 2014. Relationship between low stratiform cloud amount and estimated inversion strength in the lower troposphere over the global ocean in terms of cloud types. *Journal of the Meteorological Society of Japan* **92**: 107–120, doi: 10.2151/jmsj.2014-107.

Medeiros B, Stevens B, Bony S. 2015. Using aquaplanets to understand the robust responses of comprehensive climate models to forcing. *Climate Dynamics* **44**(7–8): 1957–1977, doi: 10.1007/s00382-014-2138-0.

Norris JR. 1998a. Low cloud type over the ocean from surface observations. Part I: relationship to surface meteorology and the

vertical distribution of temperature and moisture. *Journal of Climate* **11**: 369–382, doi: 10.1175/1520-0442(1998)011<0369:LCTOTO>2.0.CO;2.

Norris JR. 1998b. Low cloud type over the ocean from surface observations. Part II: geographical and seasonal variations. *Journal of Climate* **11**: 383–403, doi: 10.1175/1520-0442(1998)011<0383:LCTOTO>2.0.CO;2.

Norris JR, Klein SA. 2000. Low cloud type over the ocean from surface observations. Part III: relationship to vertical motion and the regional surface synoptic environment. *Journal of Climate* **13**: 245–256, doi: 10.1175/1520-0442(2000)013<0245:LCTOTO>2.0.CO;2.

Sugimoto S, Sato T, Nakamura K. 2013. Effects of synoptic-scale control on long-term declining trends of summer fog frequency over the pacific side of Hokkaido Island. *Journal of Applied Meteorology and Climatology* **52**(10): 2226–2242, doi: 10.1175/JAMC-D-12-0192.1.

Tanaka HL, Ishizaki N, Nohara D. 2005. Intercomparison of the intensities and trends of Hadley, Walker and Monsoon Circulations in the Global Warming Projections. *SOLA* **1**: 77–80, doi: 10.2151/sola.2005-021.

Tanimoto Y, Xie SP, Kai K, Okajima H, Tokinaga H, Murayama T, Nonaka M, Nakamura H. 2009. Observations of marine atmospheric boundary layer transitions across the summer Kuroshio extension. *Journal of Climate* **22**: 1360–1374, doi: 10.1175/2008JCLI2420.1.

Taylor KE, Stouffer RJ, Meehl GA. 2012. An overview of CMIP5 and the experiment design. *Bulletin of the American Meteorological Society* **93**(4): 485–498, doi: 10.1175/BAMS-D-11-00094.1.

Teixeira J. 1999. Simulation of fog with the ECMWF prognostic cloud scheme. *Quarterly Journal of the Royal Meteorological Society* **125**: 529–552, doi: 10.1002/qj.49712555409.

Warren SG, Hahn CJ, London J, Chervin RM, Jenne RL. 1988. *Global Distribution of Total Cloud Cover and Cloud Type Amounts Over the Ocean, NCAR/TN-317+STR*. National Center for Atmospheric Research: Boulder, CO.

Webb MJ, Lock AP. 2013. Coupling between subtropical cloud feedback and the local hydrological cycle in a climate model. *Climate Dynamics* **41**(7–8): 1923–1939, doi: 10.1007/s00382-012-1608-5.

Webb MJ, Lock AP, Bodas-Salcedo A, Bony S, Cole JNS, Koshiro T, Kawai H, Lacagnina C, Selten FM, Roehrig R, Stevens B. 2014. The diurnal cycle of marine cloud feedback in climate models. *Climate Dynamics* **44**: 1419–1436, doi: 10.1007/s00382-014-2234-1.

Winker DM, Vaughan MA, Omar AH, Hu Y, Powell KA, Liu Z, Hunt WH, Young SA. 2009. Overview of the CALIPSO mission and CALIOP data processing algorithms. *Journal of Atmospheric and Oceanic Technology* **26**: 2310–2323, doi: 10.1175/2009JTECHA1281.1.

Yukimoto S, Yoshimura H, Hosaka M, Sakami T, Tsujino H, Hirabara M, Tanaka TY, Deushi M, Obata A, Nakano H, Adachi Y, Shindo E, Yabu S, Ose T, Kitoh A. 2011. Meteorological Research Institute Earth System Model Version 1 (MRI-ESM1) – model description. *Technical Reports of the Meteorological Research Institute* **64**: 83. http://www.mri-jma.go.jp/Publish/Technical/index_en.html (accessed: 12 August 2016).

Yukimoto S, Adachi Y, Hosaka M, Sakami T, Yoshimura H, Hirabara M, Tanaka TY, Shindo E, Tsujino H, Deushi M, Mizuta R, Yabu S, Obata A, Nakano H, Koshiro T, Ose T, Kitoh A. 2012. A new global climate model of Meteorological Research Institute: MRI-CGCM3 – model description and basic performance. *Journal of the Meteorological Society of Japan* **90A**: 23–64.

Zhang M, Bretherton CS, Blossey PN, Austin PH, Bacmeister JT, Bony S, Brient F, Cheedela SK, Cheng A, Del Genio AD, De Roode SR, Endo S, Franklin CN, Golaz J-C, Hannay C, Heus T, Isotta FA, Dufresne J-L, Kang I-S, Kawai H, Köehler M, Larson VE, Liu Y, Lock Adrian P, Lohmann U, Khairoutdinov MF, Molod AM, Neggers RAJ, Rasch P, Sandu I, Senkbeil R, Siebesma AP, Siegenthaler-Le Drian C, Stevens B, Suarez MJ, Xu K-M, von Salzen K, Webb MJ, Wolf A, Zhao M. 2013. CGILS: results from the first phase of an international project to understand the physical mechanisms of low cloud feedbacks in single column models. *Journal of Advances in Modeling Earth Systems* **5**(4): 826–842, doi: 10.1002/2013MS000246.